Title of Invention: 3D Printed Ultrasonic Probes and Lenses for Nondestructive Testing

Description of the Invention

1.1. Background

. The use of nondestructive testing(NDT) during the production, construction and service stages of many industries, is both invaluable and unavoidable. However, the costs involved in the usage of NDT technology are often rather high and require skilled judgement and adequate experience for precise and accurate measurements. NDT equipment and artificially produced test specimens for research purposes are often costly and require much time and effort for produce. In this study, we focus on Ultrasonic Testing (UT), one of the most commonly used inspection method in industries. Probes and transducers also require precision and accuracy to produce precise guided ultrasonic waves for UT.

It is, however, not impossible to reduce cost and yet retain the same level of precision required for such UT equipment mentioned. Additive manufacturing (AM), first surfaced in 1987 with the development of Stereolithography (SLA) by 3D systems, may provide such an alternative to the current production methods.[1] The growing use of AM, or also well known as 3D printing, throughout various industries in the world can be attributed to the relatively low costs in precision products and the reduction of production time.
In this study, we combine the efficiency and effectiveness of AM methods to produce equipment and flawed specimens commonly used in Ultrasonic testing for the purposes of investigating the possibility of production using 3D printing.

1.2. Objectives

The primary objective of this study is to analyse the usability of products commonly used in NDT procedures fabricated with various 3D printing techniques.

2 Probe Design

Two types of probes were produced using FDM printing with ABSplus material, namely the angled beam and focused immersion probes. Here describes the methods and considerations used to obtain suitable designs of the probes before fabrication using 3-D printing.

2.1 Angled Beam Probe

This section discusses the considerations taken and the respective calculations used to determine a finalized design of the angled-beam probe that is to be fabricated with the following specifications.

Table 1Required Specifications for fabrication of Probe

Material used	ABS plus
Method of print	Fused Deposition Modelling (FDM)
Printer used	Stratasys DimensionElite
Material to be tested on	Carbon Steel

2.1.1Considerations

In the design of an angled beam probe, specific requirements must be met. These requirements will be discussed in detail below, and the respective calculations made to determine a finalised design.

From the Figure, $V_{i(Long)}$ is the velocity of the longitudinal ultrasonic wave incident to the planar surface of the test material, V_r is the refracted wave in the test material, V_{ref} is the reflected wave from the surface plane of the test material. The following considerations take reference to Figure 1above.

It is to note that the following calculations in this section for the determination of a suitable probe angle is made for the conditions, taking Carbon Steel as a reference test material, in Table 2.

Table 2 Conditions for determination of probe angle

Longitudinal Velocity of ABSplus (Experimentally obtained)	1783 m/s
Shear Wave Velocity of Carbon Steel, $V_{r(Shear)}$	3230 m/s
Longitudinal Velocity of Carbon Steel, $V_{r(Long)}$	5890 m/s
Transducer Frequency Used	1.0 MHz

According to Snell's Law, the incident wave will be refracted when there is a change in velocity due to different material properties. In this case, the ultrasonic waves are travelling from a slower medium to a faster medium and hence the angle of incidence would be smaller than the angle of refraction.[2] As elaborated in the Literature Review, the refracted waves are a mixture of longitudinal and shear waves refracted at different angles. Therefore, it is vital to isolate the shear waves as much as possible to refrain from obtaining multiple readings.

To ensure the shear waves are isolated and no longitudinal waves are refracted within the material, the first critical angle is to be obtained using Snell's Law below. The following calculations are taken with reference to Figure 2.

The First Critical Angle, θ_{C1}, occurs when the refracted longitudinal wave is parallel to the surface of the test material. Hence, $\theta_3 = 90°$.

Using Snell's Law,

$$\frac{sin\Theta_{c1}}{v_{i(Long)}} = \frac{sin\Theta_3}{v_{r(long)}}$$

$$\frac{sin\Theta_{c1}}{1783^0} = \frac{\sin(90^0)}{5890} \qquad \Theta_{c1} = 17.62^0$$

The Second Critical Angle indicates the maximum angle of the Probe that allow for shear waves to pass through. It occurs when $\theta_2 = 90°$ and is calculated according to the equation as follows.

$$\frac{sin\Theta_{c2}}{i(Long)} = \frac{\sin\Theta_2}{v_{r(Shear)}}$$

Therefore, it is required that $17.62° \leq \theta_1 \leq 33.02°$.

2. Use of Snell's Law to obtain suitable angle of Probe

With the critical angles as a limit for the angle that can be used, the following calculations are made to be able to get a refracted angle of approximately 50° in the steel specimen.

With reference to Figure 3, since the angle of probe, $\theta_P = \theta_i$, we may calculate the probe angle to obtain a refracted angle, θ_2 of 50°.

Taking into consideration that $17.62° \leq \theta_1 \leq 33.02°$, hence for $\theta_2 = 50°$,

Therefore, it is required for the probe angle to be approximately 25°.

3. Internal Reflections within Probe

With reference to Figure 1 above, there would be internal reflections within the probe which would possibly result in additional signals received by the transducer. Hence, it is vital for the probe to be able to absorb and reflect away these unwanted signals from the transducer to allow the readings taken to be clear and accurate.

2.1.2 Final Design of Angled Beam Probe

With the aforementioned considerations, the finalised design was selected to be as follows.

Angle of Probe	25°
Selected Design	Probe with Horn

Therefore, with the above selections, the design of the probe is shown in Figure 6

2.2 Focused Immersion Probe

Focused probes are valuable tools in ultrasonic testing for immersion tests. By using a probe to focus the ultrasonic waves, sensitivity and resolution levels can be enhanced.[3] This section describes the considerations and method taken to develop a suitable design for the focused probe.

2.2.1 Acoustic Parameters

The acoustic parameters that are taken into consideration in the development of the focused probe design are listed below.

Table 3 Acoustic Parameters [18]

Acoustic Parameters	Formula
Nearfield Distance, N	$N=\frac{D^2}{4V_W}f$
Acoustical Focal Length, F_a	$F_a= R_l 1/[(1-V_W/V_l)+\lambda(k/r)]$,$k=R_l/r$
Geometric Focal Length,F_g	$F_g=R_l/[1+(V_W/V_l)(\frac{1}{k})^2]/(1-\frac{V_W}{V_l})$
Focal Diameter d ,	
Focal Zone Length, l	$l = 4\lambda(\frac{F_a}{2r})^2$
Water Path,L L	

A preliminary assessment of design feasibility is conducted as a first step to the development of probe design.[2] Two factors are considered here: that the acoustic focal distance should be significantly shorter than the near-field distance and that the focal zone diameter has to be smaller than the minimum flaw size. With this, two stages of the assessment for feasibility of probe fabrication are as follows:

1. $F_a \leq 0.7$ N
2. $d = \frac{1}{2}$ of beam diameter at near-field distance of the selected transducer

For stage 1, the near-field distance and probe diameter for the various available transducer frequencies are presented in Figure 8 below.

Thence, focussing effects may occur only for positions along the sound path within the near-field zone if a flat probe has a specific maximum natural focal length.[4]

The next stage of the preliminary assessment requires a comparison of flat face transducer beam diameter and desired focal zone diameter.

At Fresnel (or Near-Field) zone, the beam converges for a flat face transducer, as observed in Figure 9. For a flat probe, the last interference peak in the Fresnel Zone is determined by the near-field distance, after which the pressure reduces steadily along the beam axis. This point has the smallest diameter at the 6dB drop in the direction perpendicular to the beam propagation.

The beam diameter at the focal zone for a circular element, also known as the "spot size" may be estimated from the following equation:

$$BD_{-6dB} = \frac{1.02F_a}{fD} V_{lens}$$

This equation can be simplified to obtain: $BD_{-6dB} = 0.2568 D S_F$

where, S_F = Normalized Focal Length (For flat transducers, S_F = 1)

BD_{-6dB} = Beam Diameter at the 6dB drop boundary

Thus we may obtain the following relationship of the diameters of flat face transducer and their respective spot sizes in Figure 10.

2.2.2 Design Development and Calculations

The design development and appropriate calculations required are discussed . As the focussing effect of the probe is an essential factor in producing such probes, this study tests the focussing effects of the 3D printed probe. Hence, to determine the required values to be facilitate the experiment, the following specifications have been selected.

Water Path, L = F_a = 40mm

Velocity in Water, V_W = 1493m/s

Velocity in Probe, V_l = 1901m/s

Table 4 Specifications of available transducers

Specifications of transducer	
Frequency, f (MHz)	5.0
Radius, r (mm)	5.5

In water, the geometric focal distance, F_g is approximated using the equation as follows:

$$F_g = R_l \times K_g$$

From Fig.11 below, k =R_l/r, hence the correlation is determined.

The respective properties of potential designs of focused probe in water for the above listed transducers are hence calculated in Table 5 below:

Table 5.Calculated acoustic properties with various transducer frequencies

Parameters	Values
Frequency, f (in MHz)	5.0
Radius, r (in mm)	5.5
k	2.5
K_g	13.37
Wavelength, λ (in mm)	0.2986
Curvature Radius, R_l (in mm)	13.75
Geometric Distance, F_g (in mm)	183.84
Acoustic Focal Distance, F_a (in mm)	39.25
Focal Zone Diameter at the level of -6dB, d (in mm)	1.07
Focal Zone Length at the level of -6dB, *l* (in mm)	15.21

In the table, the values of k was selected to give Fa values of approximately 30mm, and K_g was derived from Figure 12.

Therefore, from the considerations as well as the calculated values, the 5MHz transducer was selected to be used with the fabricated probe. The finalized design of the probe would hence be as follows:

3. Experimental Phase-Feasibility of Study

FDM printed ABSplus is used for the fabrication of the probes. As FDM printing may result in high attenuation due to the relatively high levels of porosity, specimens were taken from the 3D printing centre to be tested to better understand its ultrasonic attributes. Furthermore, this validation phase ensures the reliability of the use of USM 35 as a measuring device to be used for estimates of attenuation and velocity.

3.1 Apparatus Required

1. USM 35 Machine
2. Test objects: FDM printed specimens obtained from 3-D printing centre
3. Ultrasonix Couplant
4. 0.5, 1, 2.25, 5 MHz contact transducers

3.2 Procedure

The straight beam transducers are calibrated to ensure that they may be suitably used in this phase. After which, pulse echo technique is used for most of the specimens, except for those that have very high attenuation. In such cases, through-transmission technique is used. The procedures are repeated on randomly selected parts of the test objects with the transducers of frequencies mentioned in section 6.2.1.

In addition, attenuation and velocity values are recorded as well.

To obtain attenuation values, the amplitude of the first back wall echo is raised to 100% FSH and the gain value is recorded. Next, the amplitude of the next back wall echo is raised to 100% FSH and its value is recorded as well. The attenuation would be the FSH of the second echo subtracted by that of the first echo.

To obtain material velocity, the aGAT feature is used. It is adjusted to read at 10% of the signal at 80% FSH. The velocity of ultrasound is then adjusted accordingly until the aGAT first intersects the first back wall echo at the depth of the tested area.

Therefore, the attenuation, material velocity values and waveforms recorded on USM 35 are analysed and observations are discussed under Results and Discussion.

3.3 Identification of Back wall Echoes (Finger Test)

Due to the nature of the test materials used, there may be high reflectivity and back wall echoes may be hard to identify as a result of the mixture of signals. Therefore, this test was used to ensure that the right signal was picked out.

The procedure is conducted as follows. Couplant is applied on the finger. While the transducer is still on the surface of the test object, place finger on the opposite end of where the transducer is positioned. A drop in amplitude of the back-wall echo will be observed and to be sure, lift finger off surface and the echo signal amplitude will rise back up. This phenomenon is observed because when the finger is in contact with the opposite end of the sound path, part of the acoustic energy is transmitted to the finger, resulting in lowered reflected signal from the back-wall.

4.Angled Probe Tests

This section depicts the test methodology used in detail with angled probes.

4.1 Apparatus Required

The equipment required to conduct the following tests are listed as follows:

1. USM 35 machine
2. Test objects: Weld Specimens, SLM printed Centreline Defect Specimen
3. 1.0 MHz Contact Transducer
4. FDM Printed Angled Beam Probe
5. 45° 4MHz and 45° 2MHz Angled Probes

The weld specimens used are shown in the following table.

Table 6 Weld Specimens used

Defect 2 – Root Crack	Defect 5 – Centreline Crack	Defect 11 – Incomplete Root Penetration
		

4.2 Procedure – Angled Beam Inspection Test

Calibration is first conducted using the Angled Probe Calibration Test .

Sufficient couplant is then spread on the surface of the test object, and the probe is placed on the surface in the manner as shown in Figure 13 below.

The specimen is then scanned using the following 4 sweeping movements as depicted in the Figure 14 below until a reading on the screen is observed. The %FSH and location of maximum amplitude detection are both recorded and the test is repeated using different positions of the probe as shown.

From Figure 13, the sweeping movements depicted are moving along a radial path as seen in (a) while pointing at the same spot, moving towards and away from the discontinuity such as in (b), moving side to side along the length of the discontinuity such as in (c) and turning the probe while still positioned on the same spot as shown in (c).

This test procedure was conducted using the FDM printed probe as well as industrial probes.

5. Focused Beam Probe Tests

The main objective of this stage is to test the focusing capabilities of the 3-D printed focused probe in water. There are two test procedures to determine the focussing capability of the fabricated focused probe.

5.1 Apparatus Required

The equipment required to conduct the following tests are listed as follows:

1. An empty and transparent container filled with water
2. 5.0 MHz Contact Transducer
3. Long pin with markings of 5mm apart
4. Ruler and measuring tape
5. USM 35X machine
6. FDM Printed Focused Probe

5.2 Focused beam Test

This test determines the focusing abilities of the FDM printed probe.

The pin is first attached to the bottom of the container, such that the depth of the pin is at the first marking, as seen in Figure 15. The probe is then attached to the transducer and partially submerged into the water such that water covers approximately ¾ the height of the probe. It is important to ensure that the probe height from the bottom of the container is constant and the pin is not tilted at an angle, so that maximal accuracy is attained.

For an approximation of the beam diameter at the different heights, the probe is moved slowly horizontally while its height above the pin remains constant. This is conducted as the signal from the reflector increases from a signal amplitude of 6dB lower than the maximum to the maximum signal and back to the 6dB drop in signal amplitude.

Both readings of the %FSH and the beam diameters are recorded. The test is then repeated for varying values of distance from the probe to pin head.

6 Results and Discussion

6.1 Results of Experimental Phase

This study was done with various specimen made from Stratasys DimensionElite FDM printer with ABSplus and the PolyJet. The objective of this stage is to develop a greater understanding of the ultrasonic capabilities of the potential probes to be fabricated.

6.1.1 Feasibility

In this stage, various specimens were tested and the shape of the graphs were analysed accordingly. It was observed that the major factors of attenuation relative to different samples of the same material were the following:

1. Porosity Level

The porosity level of the printed parts varied as a result of the different printing methods, different options of layer thickness that the user may select from, geometry of the parts and the different rate of cooling at different portions of the same part.

I. Relatively High Porosity Level

Parts that came under this category were FDM printed ABSplus parts that used a layer thickness of 0.254mm. These parts had very low signal strength which can be observed from Figure 16 below.

This phenomenon can be explained as the degree of scattering would be very high within parts with high porosity for the amount of voids present are higher. Printing with a larger layer thickness, compared to 0.178mm, would result in larger and more voids present because when material is extruded during the FDM process, it quickly solidifies which result in the high possibility of voids being present within the internal structure.

Relatively Low Porosity Level

Parts that came under this category included FDM printed ABSplus parts that used a layer thickness of 0.178mm and the parts printed from PolyJet. These parts had relatively stronger signal strengths due to the relatively lower degree of scattering.

2. Surface Roughness

Surface roughness proved to be a factor that affected attenuation and analysis of the A-scan results. From the Figures 17 and 18 below, it was observed that there were different amounts of signal strengths detected though the analysis was only located on a specific area of the test material. The rougher surface gave a much lower back wall echo compared to the smoother surface. This was a result of scattering occurring at the surface of the rough material, causing low transmissibility.[3] Furthermore, from the right side of Figure 17, there are a mixture of back wall echoes. This may have been due to the rough back wall of the same test specimen causing reflection signals to be deflected in different directions.

As 3D printing typically results in rougher surfaces compared to machined parts, it is important to be aware of any significant effects caused by surface roughness when analysing 3D printed parts using ultrasound.

3. The frequency of the transducer

From Figure 19, the levels of penetration reduced with increasing frequency of the transducer used. However, in terms of resolution, because of smaller wavelengths used, greater frequencies would be able to detect smaller defects.

6.1.2 Velocity and Attenuation

In the next part of the Experimental Phase, the velocity and attenuation were determined with the use of different couplants and different frequencies. This is done in preparation for the design of the angled and focused probes to decide suitable settings such as material velocity, transducers and the orientation of part when printed.

The test specimens that were used to determine velocity and attenuation values were named "O. Specimens" which were printed using FDM, with layer thickness of 0.178mm.

The averaged material velocity of the test material for each transducer used was determined as follows:

$$\bar{V}=\frac{\sum V}{n}$$

Frequency of Transducer used (MHz)	Averaged Velocity, $\bar{V}$ (m/s)
1.0	1783
5.0	1901

Attenuation and signal strength was compared between the different combinations of couplants, either oil or Ultrasonix, used and frequencies of transducer used.

The increasing frequency did lead to increasing attenuation. The 1MHz probe was selected to be used with the Angled Beam probe due to the relatively high penetration ability.

6.2 Angled Beam Probe Inspection

For the Angled Beam Probe, its effectiveness in this study is determined by the sensitivity of the probe on Carbon Steel, as well as the strength of the signals that can be picked up from the reflectors.

Firstly, calibration was done to ensure that the angled probe could work within expectations. In the first calibration check to identify the index point, it was theoretically predicted, by using the centreline of the transducer, that the index point of the FDM printed angled probe would be at the centre as shown in Figure 21.

However, it was proven otherwise. The actual index point is in fact only 15mm from point 'X' in Figure 21 rather than half the base length of the probe.

Figure

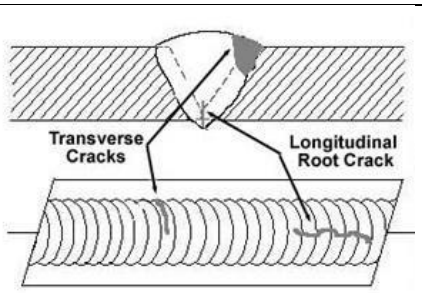
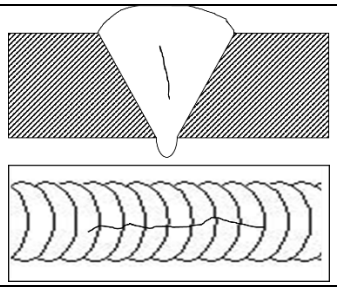
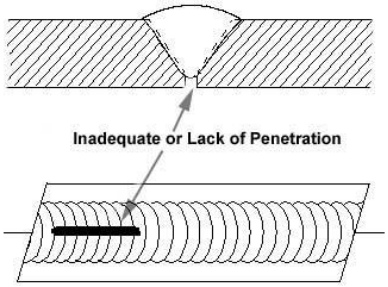
Nevertheless, the deviation was within expectations, as there are many factors that would deviate the index point such as wedge attenuation, frequency of the transducer used and size of the crystal. Brook et. al.[2] had found that the attenuation effects of the wedge play a significant role in the deviation of index point. Also, the higher the frequency of the transducer used, the larger the deviation from the theoretical point. [2] It was also noted that the non-uniform material characteristics amongst the different reference blocks could cause significant variation in attenuation and velocity measurements. Hence the exact same block was used in this study for consistency.

Next, after the distance calibration was done, the angle of the probe was validated. It was found to be approximately 50°, as previously calculated and had only a slight deviation.

However, in the sensitivity calibration, it was observed that the signal-to-noise ratio was very low, of approximately 4, as seen in Figure 24 below.

Upon completion of the calibration process, the angled probe was then used to locate defects within 3 commonly used weld specimens in the NDT industry. Simplified diagrams of the type of defects present within the weld specimens are shown in Table 7 below.

Table 7 Types of Weld Defects

Type of Defect	Diagram
Defect 2 – Root Crack[43] Follows the profile of the root pass	
Defect 5 – Internal Substrate Centreline Crack Located within the weld	
Defect 11 – Incomplete Root Penetration[43]	

Due to low signal-to-noise ratio, a rough estimation of the location of the defects could only be determined through sweeping movements of the probe and observing changes in terms of slight rises in signal amplitudes.

Fig.25 showed the FDM printed probe is not at sensitive as the industrial probe due to low signal-to –noise ratio.

6.3 Focused Immersion Probe

In this study, we analyse the focusing abilities of the 3D printed Focused Immersion Probe.

Experimentally, , it was noted that a pin with rounded tip could not return a signal and a flat tip pin had to be used due to scattering effects as a result of the shape of the reflector.

To ensure that the probe was consistently level, the reflected signal from the bottom of the container was measured before every measurement was taken from the reflector. It was ensured that whenever there were changes in water level, the reflected signal from the bottom of the container was approximately reflected in the A-scan display. Figure 26 provides a better picture of the method taken to ensure consistency.

From the graph shown below, the focal point was obtained and is approximately equal to the theoretical calculations made previously.

It also showed as the signal from the reflector increased, the signal from the back-wall was reduced until the reflector amplitude was at a maximum point while the back-wall echo disappeared due to the converging beam diameter at the near-field distance from the probe. After the focal point, indicated by the maximum amplitude of the reflector signal, the back-wall signal increased while the reflector signal decreases.

Also, before the focal point, the signal strength from the reflector was higher than after the focal point. This shows the effect at the far field distance, where the intensity of the reflected signal from the reflector drops.

The resolution of the reflected waves are higher in the far-field zone compared to the near-field zone as noted in Figure 30 which shows the reflected signal from at a point in the Fraunhofer's Zone as one such example. As observed in Figure 29, the resolution of the waves are lower in the Fraunhofer's zone. The factors that shape the beam characteristics are the probe curvature and the pressure waves. Hence the focusing effect of the probe result in more interaction between the pressure waves in the near-field, or Fresnel Zone, producing an area of highly variable amplitude.[5]The narrower beam diameter also results in a better lateral resolution compared to a point in the Fraunhofer's Zone.[6] In the Fraunhofer's Zone, the sound field diverges steadily the further it gets from the transducer. Therefore, the resolution in the Fraunhofer's Zone would be lower and the intensity of the received signals will be weaker.[7]

6.4 Observations from Printed Defects

6.4.1 Specimens with Spherical Defects

The three specimens were made with different sizes of spherical defects. From the tests, not all the defects were detectable. The spherical shape of the defects result in scattering in all directions, especially if the defect size is sufficiently small, then there may be negligible ultrasonic energy being reflected back to the transducer.

It was observed during the test that there was no defect signal to be found.

Instead, there were drops in amplitude of the back wall echo signals in the presence of the spherical defects, as observed in Figure 31. This observation proved two important concepts:

1. Scattering effects

As mentioned, due to the geometry of the defect, a significant part of the energy incident on the defect scattered instead of reflecting back.

2. Law of Conservation of Energy

There was a loss in acoustic energy that reflected back from the back wall, resulting in a drop in signal amplitude.

Furthermore, the larger the defect size, the larger the drop in amplitude, which could provide an idea on the size of the defect present. We were able to identify the specimen with the largest defect size using this method of analysis.. The location of the defects could be determined by identifying the position of the probe where the largest drop in amplitude was.

With this, we were able to rank the defect sizes correctly in ascending order:

Defect Specimen 2, Defect Specimen 1 and Defect Specimen 3.

References

1. Wohlers, T. and T. Gornet, *History of additive manufacturing.* Wohler Associates, Inc., Fort Collins, Colorado, 2012.

2. Brook, M.V., *Ultrasonic Inspection Technology Development and Search Unit Design: Examples of Practical Applications*. 2012: John Wiley & Sons.

3 Krautkrämer, J. and H. Krautkrämer, *Ultrasonic testing of materials*. 2013: Springer Science & Business Media.

1. 4.. Ginzel, E.A., *Near Field and Focusing Considerations with Wedges*. 2009: Waterloo, Ontario, Canada.

5. Rumack, C.M., S.R. Wilson, and J.W. Charboneau, *Diagnostic ultrasound vol*

1. 2005: London: Mosby, 2005.

6. Huda, W. and R.M. Slone, *Review of radiologic physics*. 2003: Lippincott Williams & Wilkins.

7 Ng, A. and J. Swanevelder, *Resolution in ultrasound imaging.* Continuing Education in Anaesthesia, Critical Care & Pain, 2011. **11**(5): p. 186-192.

Claims:

1.This is the first immersion probe manufactured by 3D printing. for application to scanning acoustic microscope.

2 Unique design of an immersion probe manufactured by 3D printing.

3.Unique design of an angled –probe manufactured by 3D printing.

4.Unique design of an angled-probe.

5.Unique design of an immersion probe.

6. The distance calibration was done, the angle of the probe was validated. It was found to be approximately 50°, as previously calculated and had only a slight deviation.

7. The larger the defect size, the larger the drop in amplitude, which could provide an idea on the size of the defect present. We were able to identify the specimen with the largest defect size using this method of analysis

8. The location of the defects could be determined by identifying the position of the probe where the largest drop in amplitude was.

9. With this, we were able to rank the defect sizes correctly in ascending order:

Defect Specimen 2, Defect Specimen 1 and Defect Specimen 3.

10. Despite the high attenuation, the angled probe could still detect certain defects within the weld specimen and there was penetration through the material into the welded specimen

11. For the immersion probe, experimentally, the focal point was obtained and is approximately equal to the theoretical calculations made previously.

12. The results showed a trend as well, whereby as the signal from the reflector increased, the signal from the back-wall was reduced until the reflector amplitude was at a maximum point while the back-wall echo disappeared. This was due to the converging beam diameter at the near-field distance from the probe

13. After the focal point, indicated by the maximum amplitude of the reflector signal, the back-wall signal increased while the reflector signal decreases.

14. Also, before the focal point, the signal strength from the reflector was higher than after the focal point. This shows the effect at the far field distance, where the intensity of the reflected signal from the reflector drops.

15. Also, the resolution of the reflected waves are higher in the far-field zone compared to the near-field zone as noted in Figure 29 which shows the reflected signal from at a point in the Fraunhofer's Zone as one such example

16. As observed in Figure 28, the resolution of the waves are lower in the Fraunhofer's zone. The factors that shape the beam characteristics are the probe curvature and the pressure waves. In this case, the focusing effect of the probe result in more interaction between the pressure waves in the near-field, or Fresnel Zone, producing an area of highly variable amplitude.[5

17. The narrower beam diameter also results in a better lateral resolution compared to a point in the Fraunhofer's Zone.[6] In the Fraunhofer's Zone, the sound field diverges steadily the further it gets from the transducer. Therefore, the resolution in the Fraunhofer's Zone would be lower and the intensity of the received signals will be weaker.[7]

18.The curvature of lens 3D printed is as designed.

19.The testings of the lens verify the lens is functioning as intended.

20.Currently nothing on the market. 3D printing will have better control of parameters.

21.Currently cannot buy a probe/lens made of 3D printing technique.

22.We reduce the problem of penetration depth and optimise the material ABSreadily for testing.

23.Normally the specimen frequency of ABS is only 0.5MHzbut now we can optimise up to 4 to 5 MHz.

24.We have more accurate control of the curvature and control of reproducibility.